

TR 65-77

AD621224

TECHNICAL REPORT NO. 65-77

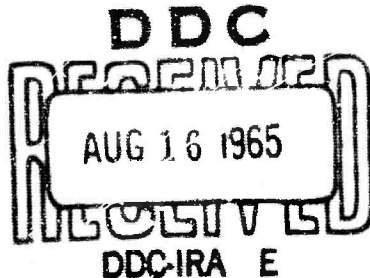
STUDY OF SHORT-PERIOD SEISMIC NOISE  
SEMIANNUAL TECHNICAL SUMMARY REPORT NO. 6  
1 January to 30 June 1965

CLEARINGHOUSE  
FOR FEDERAL SCIENTIFIC AND  
TECHNICAL INFORMATION

Barcodecopy Microfiche

\$2.00 \$0.50 40 pp as

ARCHIVE COPY



GEOTECH

THE GEOTECHNICAL CORPORATION

3401 SHILOH ROAD

GARLAND, TEXAS

**TECHNICAL REPORT NO. 65-77**

**STUDY OF SHORT-PERIOD SEISMIC NOISE  
SEMIANNUAL TECHNICAL SUMMARY REPORT NO. 6  
1 January to 30 June 1965**

---

by

**E. J. Douze  
Principal Investigator**

and

**Herbert Robertson**

Sponsored by:

The Air Force Office of Scientific Research of the  
Office of Aerospace Research under Contract AF 49(638)-1150  
as part of the Advanced Research Projects Agency's  
Project VELA-UNIFORM

**THE GEOTECHNICAL CORPORATION  
3401 Shiloh Road  
Garland, Texas**

IDENTIFICATION

AFOSR Contract No: AF 49(638)-1150

Project Title: Study of Short-Period Seismic Noise

ARPA Order Nos: 292-62, 292-63

ARPA Project Code No: 8100

Date Contract Starts: 4 April 1962

Date Contract Terminates: 15 August 1966

Amount of Contract: \$434,715

Project Scientist Name and Telephone Number: E. J. Douze, BR 8-8102

## CONTENTS

	<u>Page</u>
<b>ABSTRACT</b>	
<b>1. INTRODUCTION</b>	1
<b>2. SOME STATISTICAL MEASUREMENTS OF SEISMIC NOISE</b>	1
2.1 Introduction	1
2.2 Sampling and processing methods	2
2.3 Experimental work	3
2.4 Concluding remarks	4
2.5 References	4
<b>3. BODY-WAVE NOISE</b>	5
3.1 Theoretical background	5
3.1.1 Deep-hole array data	5
3.1.2 Surface-array data	6
3.2 Experimental results	8
3.2.1 Deep-hole array	8
3.2.2 Surface-array-experiment results	13
3.3 References	13
<b>4. FILTERED NARROW-BAND SEISMOGRAPH</b>	15
4.1 Introduction	15
4.2 System design considerations	15
4.2.1 Characteristics of signals and noise at LC-NM	15
4.2.2 Types of filters considered	18
4.3 Field testing	18
4.4 Analysis of recorded data	23
4.5 Conclusions	23
4.6 Recommendations	25
4.7 Administration	25
4.8 References	25
<b>5. HIGHER-MODE RAYLEIGH WAVES</b>	26
5.1 Discussion	26
5.2 References	29

CONTENTS, Continued

	<u>Page</u>
6. SUMMARY	29

APPENDIX - Progress report on Special Orientation Program

## ILLUSTRATIONS

<u>Figure</u>		<u>Page</u>
1	Cumulative percentage of occurrence versus absolute peak-to-peak ground displacement amplitude and percentage of occurrence versus period of P wavelets and 0.3- to 1.3-sec noise recorded by the lowest seismometer (2850 m) of the six-seismometer, deep-hole array at GV-TX	9
2	Plot of percent of occurrence versus angle of incidence $i$ (bottom) and percent of occurrence versus period for respective $i$ class intervals for P wavelets (top) recorded by six-seismometer array, GV-TX	10
3	Angle of incidence $i$ versus percent of 0.3-sec period P wavelets per $i$ class interval	11
4	Cross-correlation between seismometers at depths of 2890 and 2570 m at Grapevine, Texas	12
5	Phase angles and coherences from cross spectra between seismometers at WMSO	14
6	Plot of percentage of occurrence versus period for 8,297 P waves recorded by short-period seismographs located in a mine near LC-NM	16
7	Noise spectra at LC-NM, 8-10 June 1964	17
8	Block diagram of instrumentation used to test and evaluate the narrow-band seismographs at LC-NM	19
9	Normalized response characteristics of the seismograph systems used at LC-NM	21
10	Recording of a P phase from the New Hebrides Islands ( $\Delta = 95$ deg) by data 1-A, 1-AF, 2-B, 3-C, and 4-D seismographs at LC-NM	22

ILLUSTRATIONS, Continued

<u>Figure</u>		<u>Page</u>
11	Plot of signal-to-noise ratio versus P-wave maximum ground velocity for 30 events recorded by data 1-AF, 1-A, and 2-B seismographs at LC-NM	24
12	Theoretical amplitude-depth relationships of the first and second higher-mode Rayleigh waves, Fort Stockton, Texas	27
13	Recording of an Lg phase from Baja California, by deep-hole and surface seismographs at Fort Stockton, Texas	28

## ABSTRACT

This report describes work on short-period seismic noise, signals, and signal-to-noise ratios under Contract AF 49(638)-1150. It includes: (1) a section on statistical measurements of noise and some sampling techniques in use, (2) a section on visual and spectral techniques that were used to detect body waves in the short-period noise recorded by a deep-hole array at Grapevine, Texas, (3) a section on a filtered narrow-band seismograph that was designed to reduce noise outside the band of maximum signal information at Las Cruces, New Mexico, and (4) a section on higher-mode Rayleigh waves as recorded by deep-hole seismographs at Fort Stockton, Texas.

**BLANK PAGE**

S'1 JDY OF SHORT-PERIOD SEISMIC NOISE  
SFMIANNUAL TECHNICAL SUMMARY REPORT NO. 6  
1 January to 30 June 1965

---

1. INTRODUCTION

This report presents the results of study of short-period seismic noise, signals, and signal-to-noise ratios under Contract AF 49(638)-1150. Section 2 by Herbert Robertson discusses some statistical measurements of short-period noise. Section 3 by Eduard Douze and Herbert Robertson reports on spectral and visual analyses of P wavelets in noise as determined from deep-hole-array recordings. Section 4 discusses the filtered narrow-band seismograph that was operated at the Las Cruces, New Mexico, LRSM site. Section 5 by Eduard Douze is a discussion of higher-mode Rayleigh waves. Section 6 is a final summary. The appendix is a progress report by D. C. Ramussen on the Special Orientation Program conducted for foreign technical personnel.

2. SOME STATISTICAL MEASUREMENTS OF SEISMIC NOISE

2.1 INTRODUCTION

Some statistical measurements of short-period seismic noise are average peak noise, average noise, power spectrum (variance), and rms (root mean square or standard deviation) noise. These statistics are elementary and related (see Dixon and Massey, 1957; Longuet-Higgins, 1952; and Gumbel, 1954); however, the sampling techniques in vogue for obtaining these statistics from seismic records are somewhat involved.

Principle techniques are (a) the visual technique used in the VELA UNIFORM program, (b) the kick-sort technique used by the United Kingdom Atomic Energy Authority (UKAEA), and (c) the spectral technique used by those who have access to analog or digital processors. The respective statistics derived from these techniques are the average peak noise, average (?) noise, and variance (rms or the standard deviation is the square root of the variance).

Oceanographers such as Longuet-Higgins (1952) and Cartwright (1958) have derived mathematical relationships between the above statistics for stationary, random, narrow-band waves. Because seismologists deal with short-period noise having a bandwidth of about 3 octaves; that is, 0.3 to 1.3 sec, discrepancies may occur between statistics calculated from seismic data and those derived theoretically for ocean waves. Cartwright (1958) has calculated theoretical values of the average peak wave height and the variance for various bandwidths  $\epsilon$ ; thus, it may be possible to correct for discrepancies if they occur.

This section of the report describes briefly (a) the visual, kick-sort, and spectral methods of sampling seismic noise as well as the statistics derived from these sampling methods, and (b) a procedure for examining the relationships between the statistics and sampling methods.

## 2.2 SAMPLING AND PROCESSING METHODS

A statistic commonly used in the VELA-UNIFORM program to specify the average amplitude of seismic background noise is the average peak noise or the median of the maximum wave heights. These wave heights are peak-to-peak measurements of ground displacement amplitudes as determined from 100 samples taken from 16-mm film records (The Geotechnical Corporation, 1964, p. 15). For the determination of this statistic, the largest noise amplitudes in millimeters in the band of 0.3 to 1.3 sec present in a 10-sec interval following a 5-min mark are measured and arranged into amplitude class intervals. Magnifications at 1 Hz are used to obtain ground displacements in millimicrons. These arranged data are then plotted as cumulative percentage of occurrence versus ground displacement amplitude (see Douze, 1964, p. 722, figure 1). The median of the highest wavelets is then determined from the cumulative curve.

The United Kingdom Atomic Energy Authority (UKAEA) uses a machine technique known as the kick-sort method. The kick-sorter was originally developed for scintillation counting in nuclear research. An analog filter is used to limit the bandwidth before noise measurements are made. Cutoff points of the filter are 1 and 2 Hz, and cutoff rates are about 40 dB. A 1-min sample of typical noise is chosen, then the amplitude of the noise is sampled 100 times per sec. Amplitude samples are sorted in 97 different amplitude levels, then a cumulative curve is plotted (Hamilton, personal communication, and Carpenter, 1965, p. 366, figure 4). The median as determined from such a curve may be a measure of the average noise.

The power spectrum of a seismic record is the distribution of variance as a function of frequency (Ward, 1960, p. 23'0, and Blackman and Tukey, 1956, p. 86). Theoretically, the statistical variance of a normal distribution is the power spectral density function (Bendat, 1956, p. 101, eq. 3-65). The power spectrum (variance) of a seismic record is computed using digital processors by obtaining the autocorrelation function, taking its Fourier cosine transform, and smoothing. (See Blackman and Tukey, 1958, for a comprehensive discussion of power spectra; Longuet-Higgins, 1962, for a discussion of visual properties of the Gaussian noise record; and Grabbe, Ramo, and Woolridge, 1959, ch. 3, for a discussion of analog methods of measuring noise characteristics.)

### 2.3 EXPERIMENTAL WORK

Experimental work is underway to (a) relate visual, average, peak noise with visual, average noise, (b) relate visual estimates of variance with spectral estimates of variance, and (c) determine if any discrepancies are caused by variations in bandwidth  $\epsilon$ .

For the first experiment, we will (a) sample peak-to-peak wavelets and wavelets chosen randomly, using deep-hole seismograms from Apache, Oklahoma (AP-OK), Eureka, Nevada (EK-NV), and Grapevine, Texas (GV-TX), (b) calculate the ratio of average peak noise to average noise, and (c) compare observed ratios with theoretical ratios derived by Longuet-Higgins (1952) for narrow-band ocean waves. Preliminary results show that observed ratios for the sites considered are about 2 to 1, which agree with theoretical ratios.

For the second experiment, we will (a) obtain the power spectrum of recording from the above sites, and (b) compare the integrated power spectrum, which is the variance of the recordings, with the variance calculated from visual measurement of the same recordings.

For the third experiment, we will (a) get an accurate estimate of  $\epsilon$  from the power spectrum of each recording, (b) enter Cartwright's (1958) tables with  $\epsilon$  to obtain a ratio of the average peak noise to the rms noise, and (3) compare the resulting ratios with respective ratios calculated from mean-to-peak observations.

## 2.4 CONCLUDING REMARKS

The experimental work is being done by Herbert Robertson, geophysicist, of Geotech and William T. Tucker, statistician, of the Dallas Seismological Observatory at Southern Methodist University. Consultants are Dr. Eugene Herrin, associate professor, of Southern Methodist University and Dr. Eduard Douze, senior scientist, of Geotech. The results of this work will be reported by Herbert Robertson and William T. Tucker.

## 2.5 REFERENCES

- Bendat, J. S., 1958, Principles and applications of random noise theory: New York, Wiley & Sons, 431 p.
- Blackman, R. B., and Tukey, J. W., 1958, The measurement of power spectra: New York, Dover Publications, 190 p.
- Carpenter, E. W., 1965, Explosion seismology: Science, vol. 147, no. 3656, p. 363-373.
- Cartwright, D. E., 1958, On estimating the mean energy of sea waves from the highest waves in a record: Royal Society London Proc., Series A, vol. 247, no. 1248, p. 22-48.
- Dixon, W. J., and Massey, F. J., Jr., 1957, Introduction to statistical analysis: New York, McGraw-Hill, 488 p.
- Douze, E. J., 1964a, Signal and noise in deep wells: Geophysics, vol. 29, no. 5, p. 721-732.
- Geotechnical Corporation, 1964, Deep-well site report Perdasofpy No. 1 well, Comanche County, Oklahoma: TR 64-33, Project VT/1139, Contract AF 33(600)-43369, 38 p.
- Grabbe, E. M., Ramo, Simon, and Woolridge, D. E. (eds.) 1959, Handbook of automation, computation, and control, vol. 2: New York, Wiley & Sons.
- Gumbel, E. J., 1954, Statistical theory of extreme values and some practical applications: National Bureau of Standards, Applied Mathematics Ser. 33, 51 p.

Longuet-Higgins, M. S., 1952, On the statistical distribution of the heights of sea waves: Jour. Marine Research, vol. 11, no. 3, p. 245-266.

Longuet-Higgins, M. S., 1962, Some simple visual properties of a Gaussian noise record in Problems in seismic background noise: VESIAC Advisory Rept. 4410-32-X, p. 34-44.

Ward, F. W., Jr., 1960, The variance (power) spectra of  $C_i$ ,  $K_p$ , and  $A_p$ : Jour. Geophys. Research, vol. 65, no. 8, p. 2359-2373.

### 3. BODY-WAVE NOISE

Recent studies of short-period seismic noise strongly indicate the possibility that body-wave noise predominates in the noise of periods less than 2.0 sec at quiet locations. Studies are presently in progress to attempt to verify this theory. Preliminary results of these studies are presented in this section. The data used was obtained from the Deep-Hole Program (VT/5051) and the Array Program (VT/4054). Both visual and spectral analysis techniques are being employed.

#### 3.1 THEORETICAL BACKGROUND

##### 3.1.1 Deep-Hole Array Data

A vertical array of deep-hole seismometers can be used to visually detect body waves in the noise. Body-wave noise will show a time "step-cut" between seismometers, while surface-wave noise will not. With knowledge of the time it takes a P wave to travel between seismometers at vertical incidence, the angle of incidence can be calculated from the relationship:

$$\Delta t = \frac{\Delta Z}{V} \cos \theta$$

where  $\Delta Z$  is the distance between seismometers,  $V$  is the average P-wave velocity in the interval from the sonic log, and  $\Delta t$  is the measured time difference.

The same information can be obtained as an average over a large noise sample by cross-correlating the time series between two deep-hole seismometers. If surface waves predominate in the noise, the cross-correlation will be a maximum at zero lag; however, if body waves predominate, the maximum value will not be at zero lag, but at a lag corresponding to the average up-hole time.

It must be pointed out that the cross-correlations are difficult to interpret quantitatively. This technique will determine the presence of body waves, but it is not possible to calculate the ratio of body-wave to surface-wave noise, nor the exact frequencies at which body waves are present. The technique being followed at present is to narrow-band filter before cross-correlating; in this way, the frequencies at which body-wave noise predominate can be determined.

### 3.1.2 Surface-Array Data

Experimental data from arrays usually indicate that the noise is essentially omnidirectional, i.e., arriving with approximately equal energy content from all directions. For the case of surface waves, the solution that would be obtained has been solved by Backus et al., (1964). The spectrum of each seismometer is the same,  $\psi(\omega)$ , and the cross spectra become

$$\psi_{12}(\omega) = \psi(\omega) J_0\left(\frac{\omega \Delta x}{v}\right) \quad (1)$$

where the  $\Delta x$  and  $v$  are, respectively, separation between seismometers and phase velocity.

This solution can easily be extended to more than one wave type and results in the sum of Bessel functions equal to the number of wave types present.

Because of the possible presence of body-wave noise, it is necessary to also consider the case of body waves from random directions and random angles of incidence.

For P waves arriving at the surface seismometers with equal energy content from random directions and all angles of incidence, the time series for a vertical-motion seismometer (designated by No. 1) is

$$X_1(t) = \sum_1^N f_n(t) \cos \theta_n$$

At seismometer No. 2, the time series becomes

$$X_2(t) = \sum_1^N f_n(t - \frac{\Delta x}{v} \sin \theta_n \cos \xi_n) \cos \theta_n$$

where  $\theta$  refers to the angle of incidence, and  $\xi$  to the direction of the waves. By letting N approach infinity, the cross spectrum becomes

$$\varphi_{12}(\omega) = \varphi(\omega) \cdot \frac{1}{2\pi} \cdot \frac{1}{\pi} \int_{-\pi/2}^{2\pi \pi/2} e^{-i\omega(\frac{\Delta x}{v} \sin \theta \cos \xi)} \cos^2 \theta \cdot r \cdot d\theta$$

by performing the last integration, the expression reduces to

$$\varphi_{12}(\omega) = \varphi(\omega) \frac{1}{2\pi} \int_0^{2\pi} \frac{J_1(\frac{\omega \Delta x}{v} \cos \xi)}{\frac{\omega \Delta x}{v} \cos \xi} \cdot d\xi \quad (2)$$

where

$$\varphi_{11}(\omega) = \varphi_{22}(\omega) = \frac{1}{2} \varphi(\omega)$$

Equation 2 must be solved by numerical methods of integration.

Notice that under the assumptions made, neither formula 1 nor 2 has an imaginary part and the phase angle is either 0 or 180 deg. Equation 2 will be programmed for a digital computer. A few examples have been calculated by hand to obtain preliminary results.

In the case of waves coming from one direction (for surface waves), or one direction and angle of incidence (for body waves), the cross spectra become

$$\varphi_{12} = \varphi_{11} e^{i\omega(\frac{\Delta x}{v})} \quad (3)$$

From this equation, the cross spectral information can be solved for the apparent phase velocity (v) between seismometers.

## 3.2 EXPERIMENTAL RESULTS

### 3.2.1 Deep-Hole Array

The following visual technique was used to sample and measure incident angles of P wavelets recorded on 16-mm film by the six-seismometer array at Grapevine, Texas (GV-TX). Any wavelet in a 10-sec interval after a 5-min mark was sampled if it had moveout on four or more traces. In all, 100 wavelets were measured from recordings made in the winter of 1965. Because timing precision is thought to be about  $\pm 0.02$  sec, calculated angles will be in error about  $\pm 5$  deg for high angles and will increase to  $\pm 10$  deg as the angle approaches zero.

Figure 1 is a plot of amplitude and period data for P wavelets and for noise wavelets chosen at random. Figure 2 is a plot of percent of occurrence versus angle of incidence  $i$  (lower plot) and percent of occurrence versus period of respective class intervals for P wavelets (upper plot). The lower plot suggests a near source for most wavelets (see curves of Nuttli and Whitmore, 1961). Moreover, the upper plot shows a systematic increase in the percent of P wavelets having a period of 0.3 sec. Figure 3, a plot of angle of incidence  $i$  versus percent of 0.3-sec P wavelets, suggests that most of the 0.3-sec wavelets are generated by cultural activities close to the deep hole.

Cross-correlation techniques were also used to determine incident angles. In order to obtain the average behavior of the noise over 3 min, time series from the bottom two seismometers at Grapevine were cross-correlated. The time series were narrow-band filtered: high-pass, 3.0 Hz at 24 dB/octave; low-pass, 3.0 Hz at 24 dB/octave. This filtering ensured that the noise being investigated was the part of spectrum that at the surface consists almost entirely of first-higher-mode Rayleigh waves (Douze, 1964). Figure 4 shows the results obtained; the time lag between the seismometers indicates the presence of body waves; under the assumption that the body waves are predominantly P waves, the average angle of incidence is approximately 45 deg. This result is in good agreement with the results of visual measurements. Furthermore, the symmetry of the cross-correlation indicates that the noise is composed almost entirely of body waves. The first-higher-mode Rayleigh waves that predominate at 3 Hz at the surface have decayed with depth, and the noise at the bottom of the hole is composed of body waves and not higher-mode surface waves.

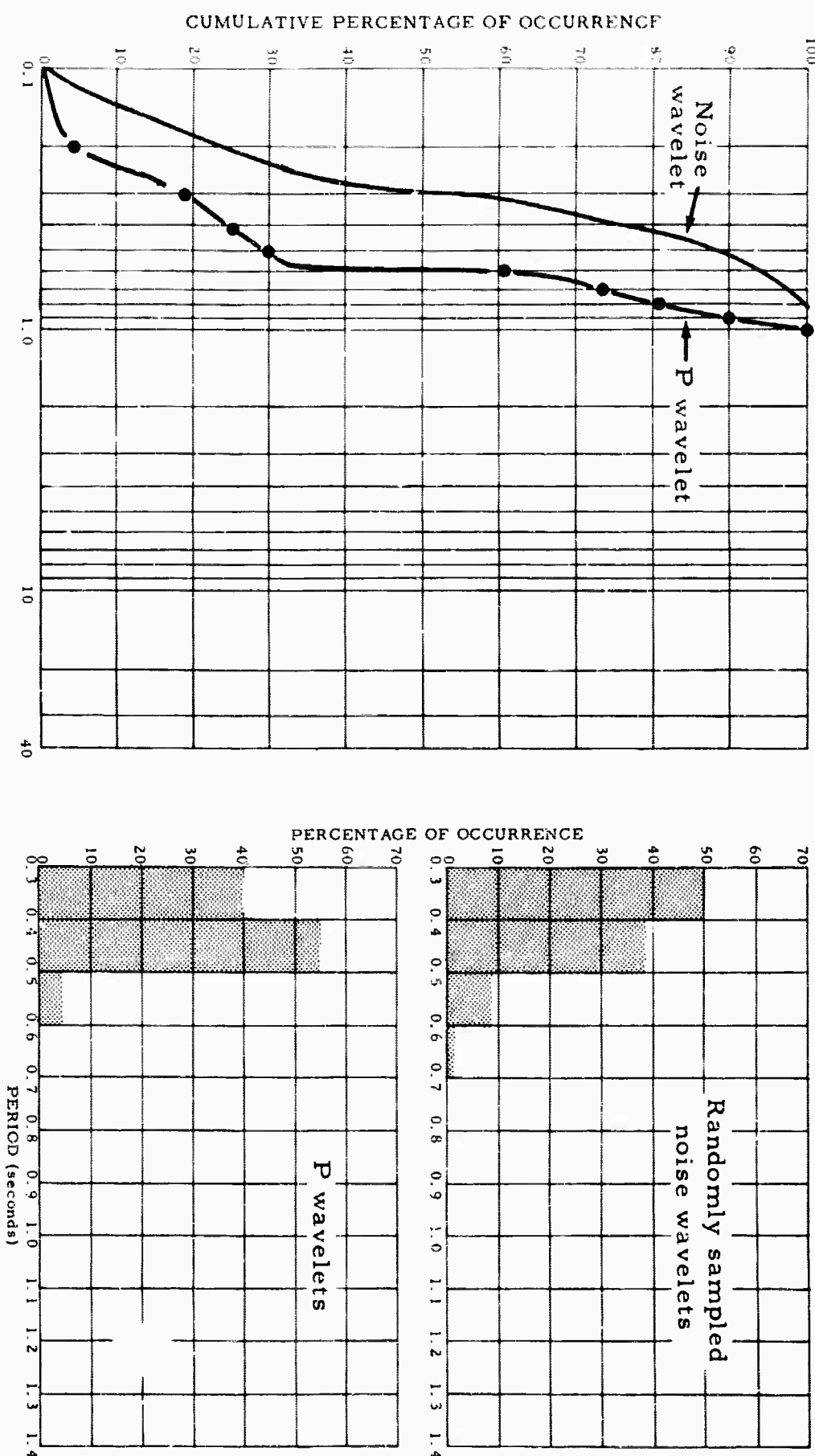


Figure 1. Cumulative percentage of occurrence versus absolute peak-to-peak ground displacement amplitude and percentage of occurrence versus period of P wavelets and 0.3- to 1.3-sec noise recorded by the lowest seismometer (2850 m) of the six-seismometer, deep-hole array at GV-TX

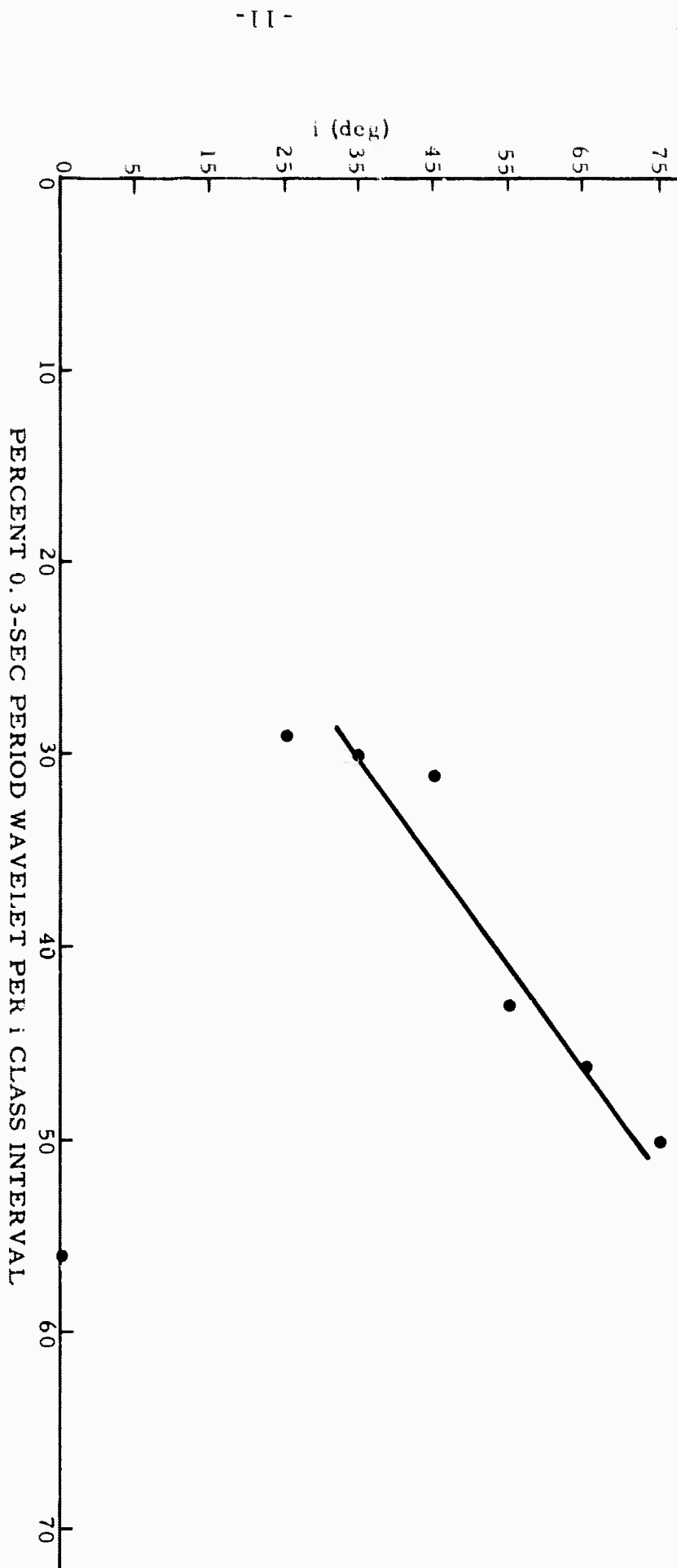


Figure 3. Angle of incidence  $i$  versus percent of 0.3-sec period P wavelets per  $i$  class interval. Regression line "eyeballed"

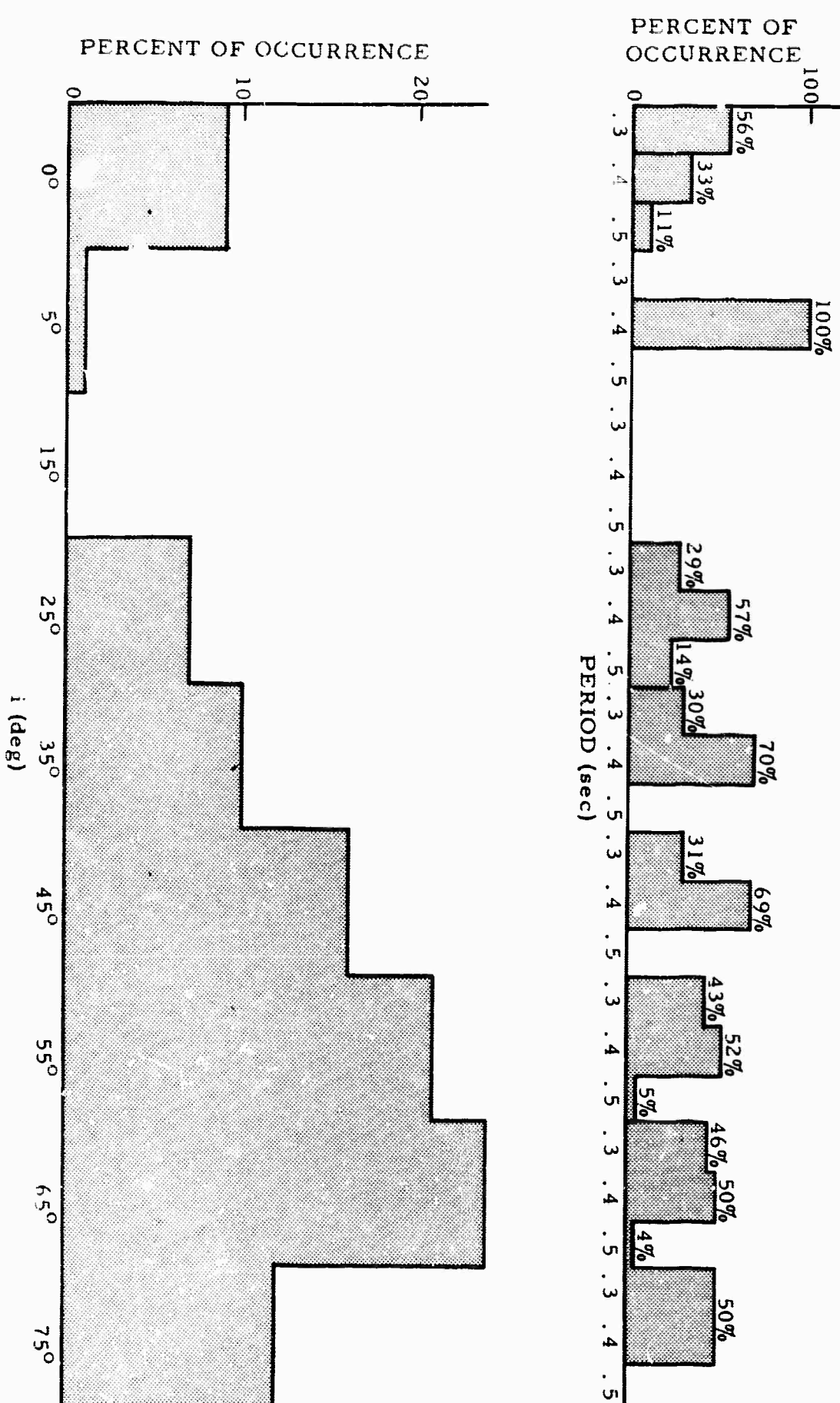


Figure 2. Plot of percent of occurrence versus angle of incidence  $i$  (bottom) and percent of occurrence versus period for respective  $i$  class intervals for P wavelets (top) recorded by six-seismometer array, GV-TX

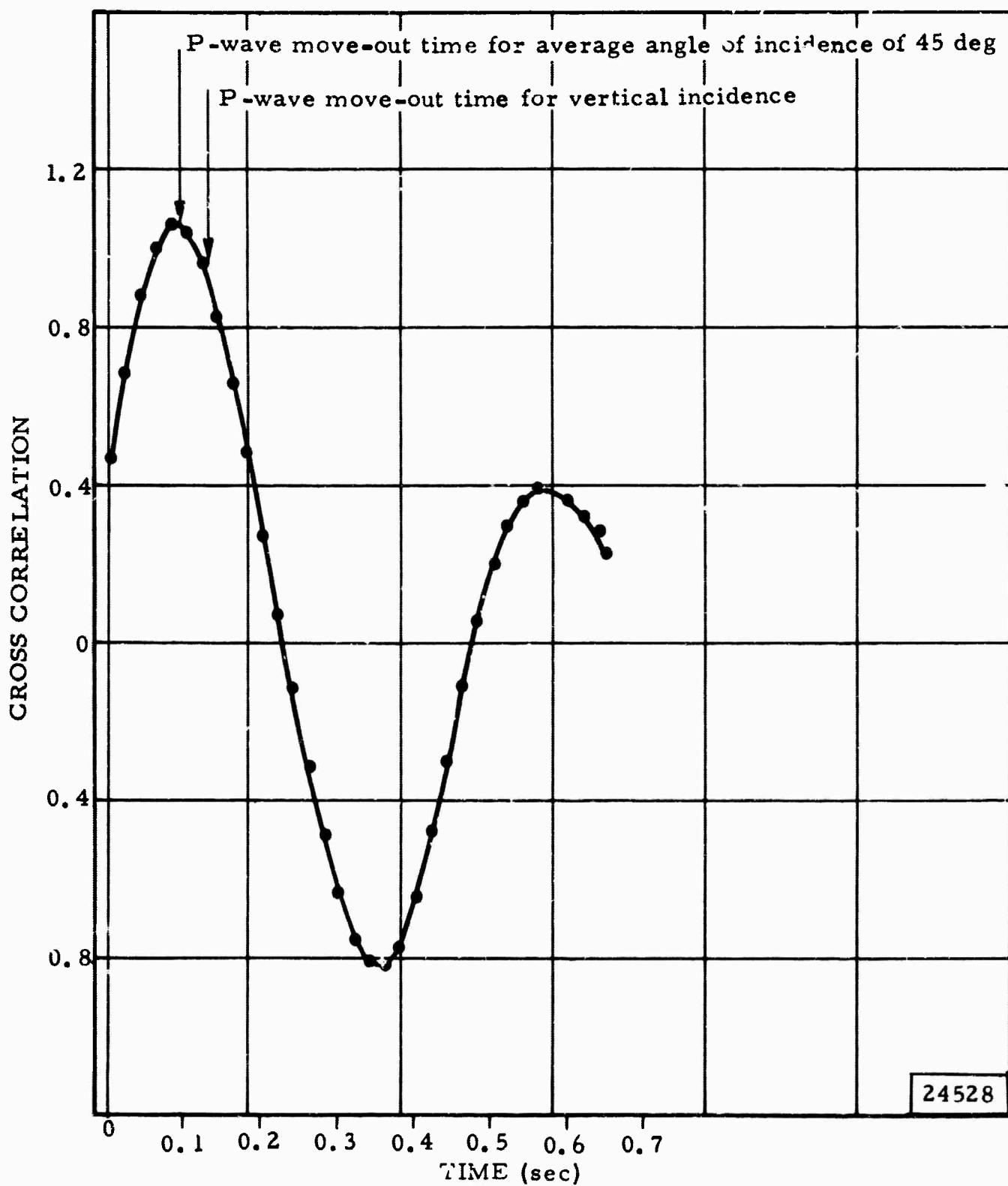


Figure 4. Cross-correlation between seismometers at depths of 2890 and 2570 m at Grapevine, Texas

### 3.2.2 Surface-Array-Experiment Results

In order to obtain phase-velocity information in an attempt to distinguish between surface- and body-wave noise, the cross spectra between Wichita Mountains Seismological Observatory (WMSO) surface seismometers at a number of spacings are being computed. Sample lengths are 3 min of noise; 8-percent lags were used; therefore, accuracy obtained for the phase angles is approximately  $\pm 25$  deg and a coherence value less than 0.8 indicates that the coherence is actually zero.

Figure 5 shows the phase angles and coherences obtained experimentally at seismometer spacings of 1.0 and 3.0 km. Although only preliminary results are available to date, a few tentative conclusions can be reached. The phase angles indicate that in general, the noise is omnidirectional by changing from 0 to 180 deg. Intermediate phase angles are obtained principally where the coherence is less than 0.7; for these low coherences, the phase angle is not meaningful and only gives random values.

The theoretical values for P-wave noise from random angles of incidence and random directions, and surface waves of 3 km/sec fall on either side of the experimental results. No firm conclusions can be drawn from the data until further analyses have been done.

### 3.3 REFERENCES

Backus, Milo, and others, 1964, Wide-band extraction of mantle P waves from ambient noise: *Geophysics*, vol. 29, p. 672-692.

Douze, E. J., 1964, Spectral analysis of seismic noise at the Perdasofpy No. 1 deep hole, Comanche Country, Oklahoma: The Geotechnical Corporation, TR 64-82, Project VT/1139, Contract AF 33(600)-43369, 17 p.

Nuttli, Otto, and Whitmore, J. D., 1961, An observational determination of the variation of the angle of incidence of P waves with epicentral distance: *Seismol. Soc. America Bull.*, vol. 51, p. 269-276

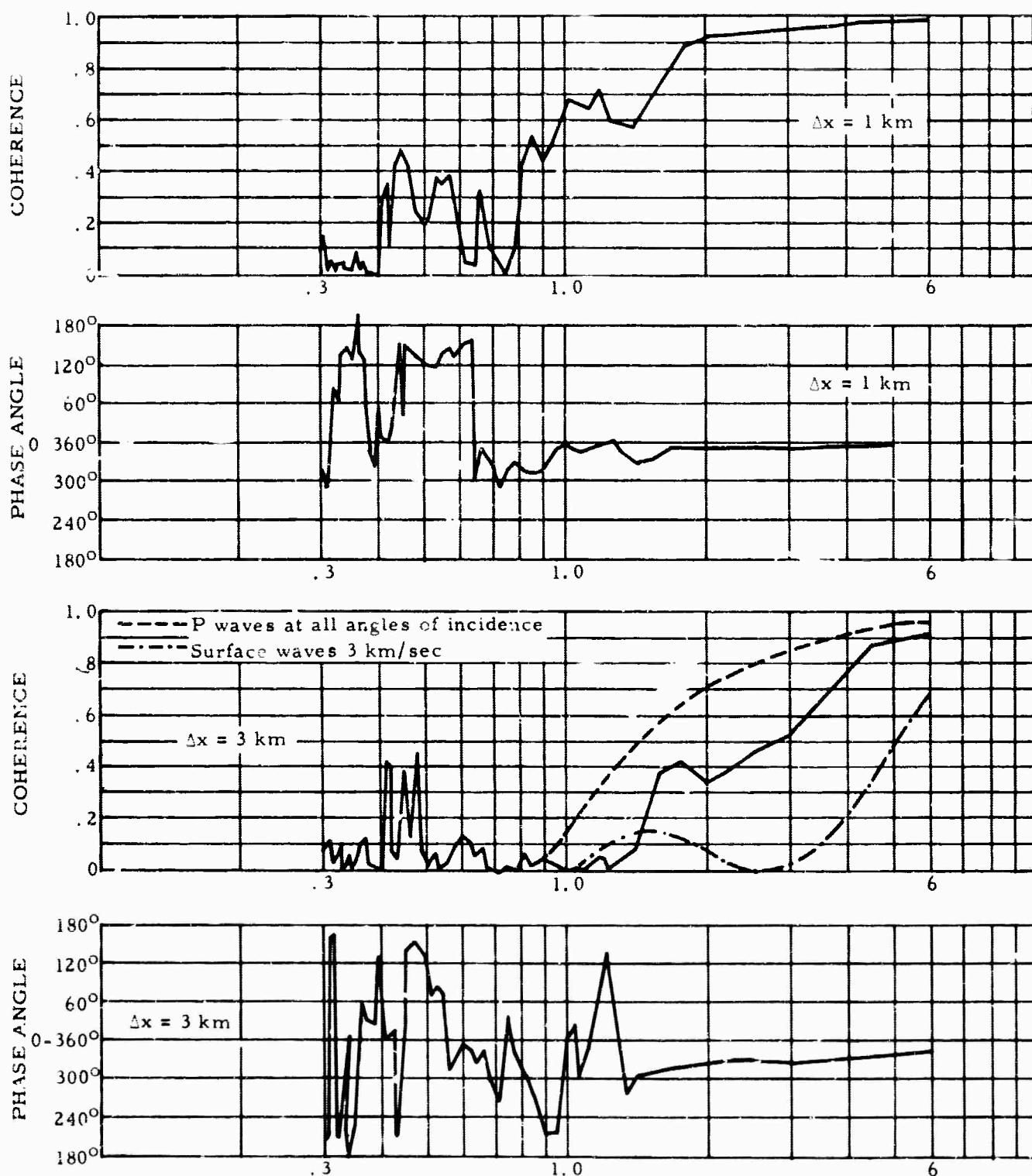


Figure 5. Phase angles and coherences from cross spectra between seismometers at WMSO

## 4. FILTERED NARROW-BAND SEISMOGRAPH

### 4.1 INTRODUCTION

This section describes a seismograph system that was designed to minimize the noise outside the band of maximum signal information at Las Cruces, New Mexico (LC-NM). The resulting system is a filtered narrow-band Johnson-Matheson (JM) vertical seismograph with a nominal passband from 0.8 to 1.0 Hz. Tests on this seismograph, along with a similar seismograph unfiltered and other broad-band vertical and horizontal seismographs, were made in a mine at LC-NM during August, September, and October 1964.

Topics covered briefly in this section are system design consideration, filters, field testing, data analysis, conclusions, and recommendations. Because Developorder records used for analysis were available for only the last 5 days of operation, conclusions are based on a limited amount of data. Detailed engineering data on steady-state, filter frequency and phase response; filter time response; and steady-state, seismometer-galvanometer-filter gain and phase response are on file if needed.

### 4.2 SYSTEM DESIGN CONSIDERATIONS

#### 4.2.1 Characteristics of Signals and Noise at LC-NM

LC-NM was originally chosen as a test site because of its low-noise level. That is, standard LRSM (Long Range Seismic Measurements Program) short-period Benioff seismographs and Noise Study broad-band systems had been operated at magnifications exceeding 1 million in the mine.

At LC-NM, the majority of the signals have periods near 1.0 sec (see figure 6). The noise level (figure 7) is near a minimum at 1.0 sec and becomes quite large at longer periods. The signal is more band-limited than the noise; therefore, a weighted transfer function that passes data relatively unreduced in the passband, a region of high signal probability, and highly reduced in the reject band, a region of low signal probability, should provide an improvement in the signal-to-noise ratio by reducing the noise more than the signal.

A seismograph with a response peaked sharply at 1 sec and bandpass filtered with steep rejection slopes on either side of 1 sec should give a maximum

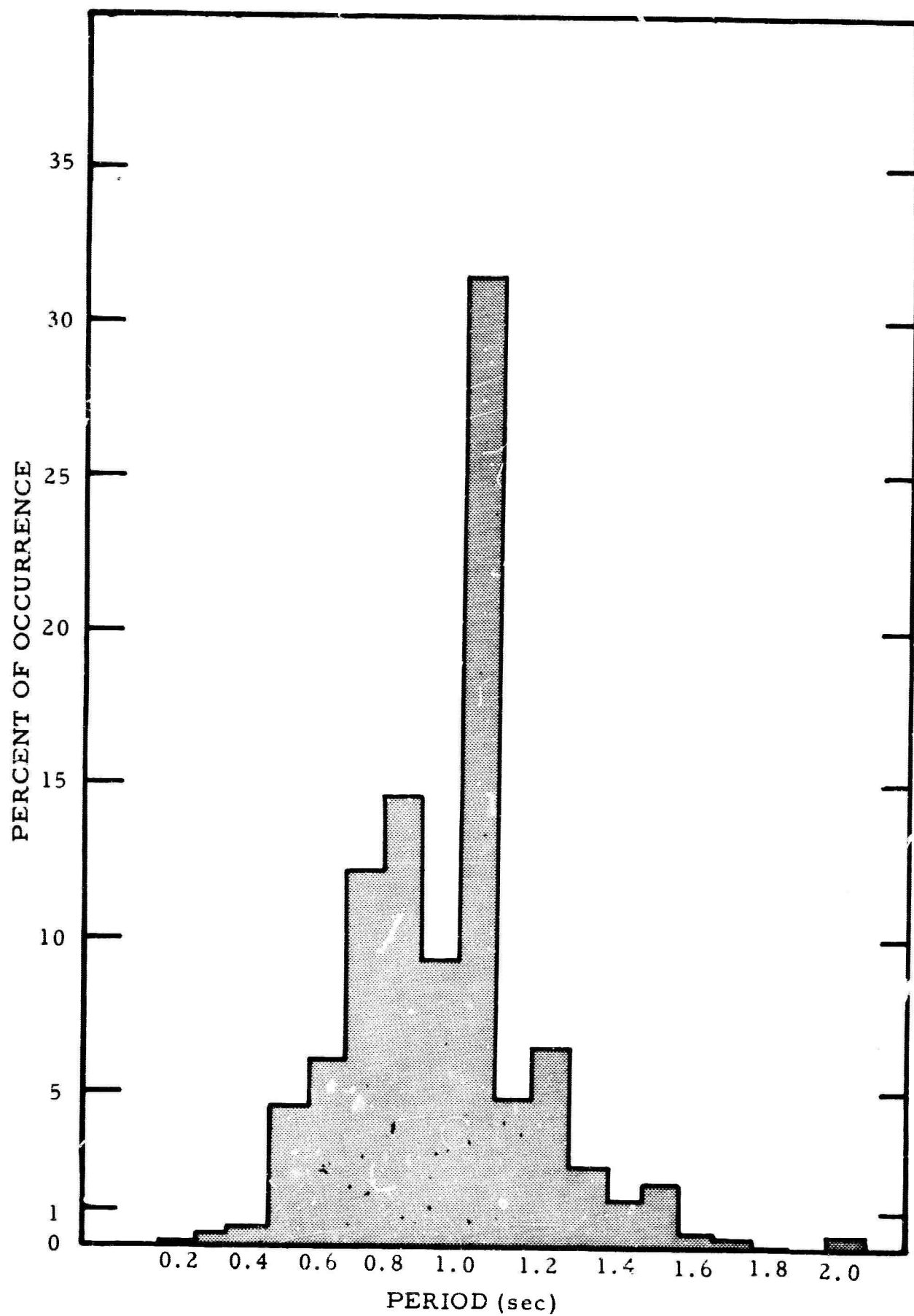


Figure 6. Plot of percentage of occurrence versus period for 8,297 P waves recorded by short-period seismographs located in a mine near LC-NM

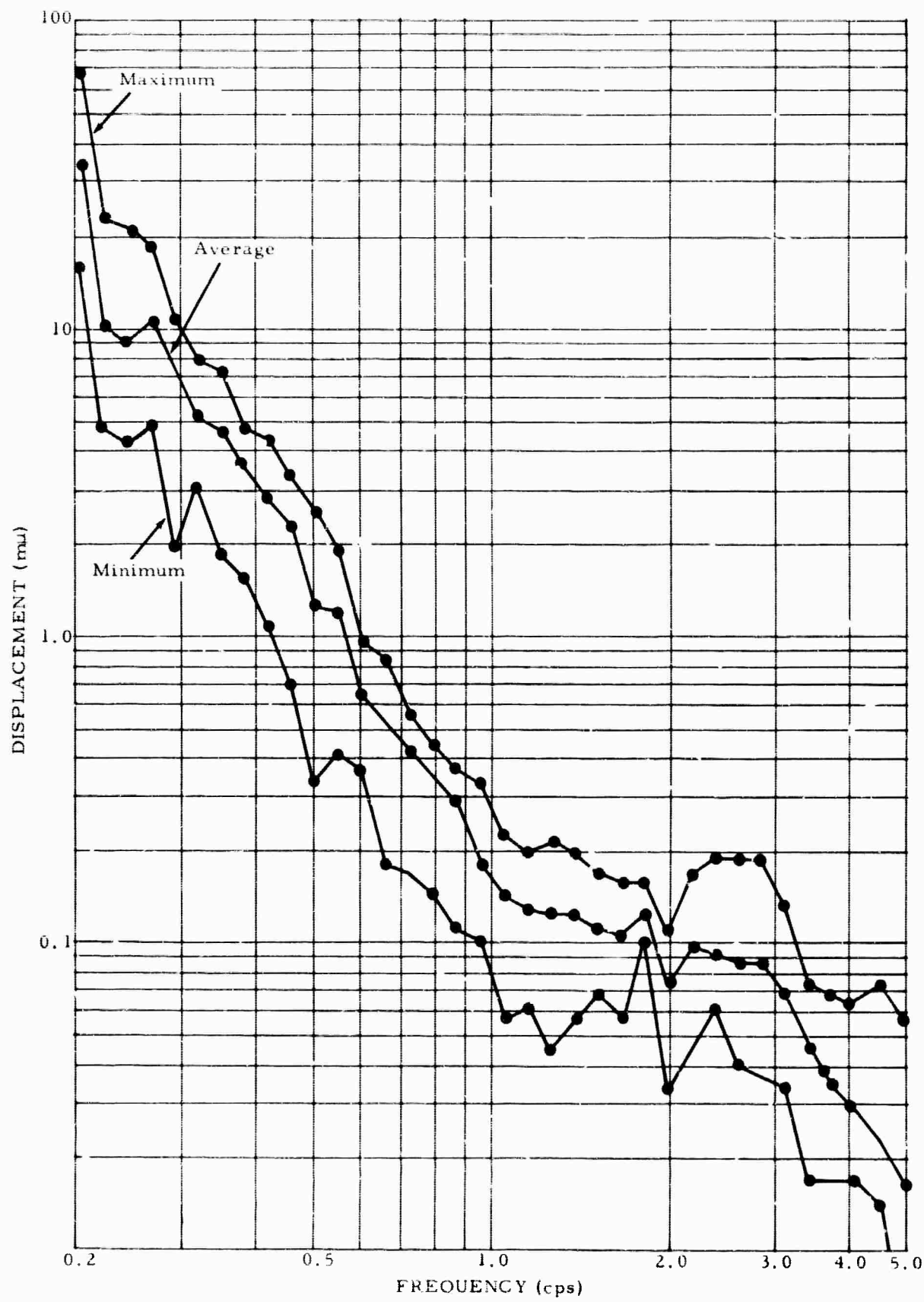


Figure 7. Noise spectra at LC-NM, 8-10 June 1964. Spectra obtained from recordings of LRSM Benioff vertical seismograph. Spectra corrected for system response.

signal-to-noise ratio at this site. The following paragraph describes briefly the types of high-pass filters considered for this seismograph. A 1-Hz galvanometer provided low-pass filtering (see figure 8).

#### 4.2.2 Types of Filters Considered

Two filters were considered: the Krohn-Hite Filter, Model 335, and the Geotech Variable Filter, Model 16307. These filters were tested in the laboratory and in field systems. Relative operational characteristics of the filters are discussed in the next section.

### **4.3 FIELD TESTING**

Instrumentation was transported by trailer to the Las Cruces, New Mexico, site. The site is an abandoned mine on the west flank of the Organ Mountains. Bedrock at the mine site is the Nakaye limestone. Seismographs were operated in the mine for a 2-week period in August 1964, and for a 3-week period in September and October 1964. On 8 October 1964, the instrumentation was returned to Geotech.

Two short-period Johnson-Matheson (JM) Vertical Seismometers, Model 6480; one Portable Short-Period (Vertical) Seismometer, Model 18300; and one (two in August tests) short-period JM Horizontal Seismometer, Model 7515, were installed on base plates in the mine approximately 10 feet from the short-period Benioff seismometers regularly used at the site by LRSM. Figure 8 shows a block diagram of the instrumentation and the channel notations used for the various seismographs. Channel notations for respective seismographs are as follows: datum 1-AF, filtered narrow-band seismograph; datum 1-A, unfiltered narrow-band seismograph; datum 2-B, broad-band JM vertical seismograph; datum 3-C, broad-band vertical Model 18300 seismograph; and datum 4-D, broad-band JM horizontal seismograph. These notations will be used to refer to respective seismographs throughout the remaining paragraphs.

Four Phototube Amplifiers (PTA's), Model 4300, were located in an underground storage room adjacent to the instrument trailer. The instrument trailer itself was located adjacent to the LRSM van. Standard carbon block and fuse lightning protectors were installed on each PTA. In addition, the datum 1-A PTA was equipped with two resistive terminating half-sections matched to its attenuator for individual seismometer-galvanometer damping adjustment. Instrument cabling, Belden 8732 four-conductor cable, was laid on the ground. Ac power leads and antenna for WWV earth grounding were installed near the instrument trailer.

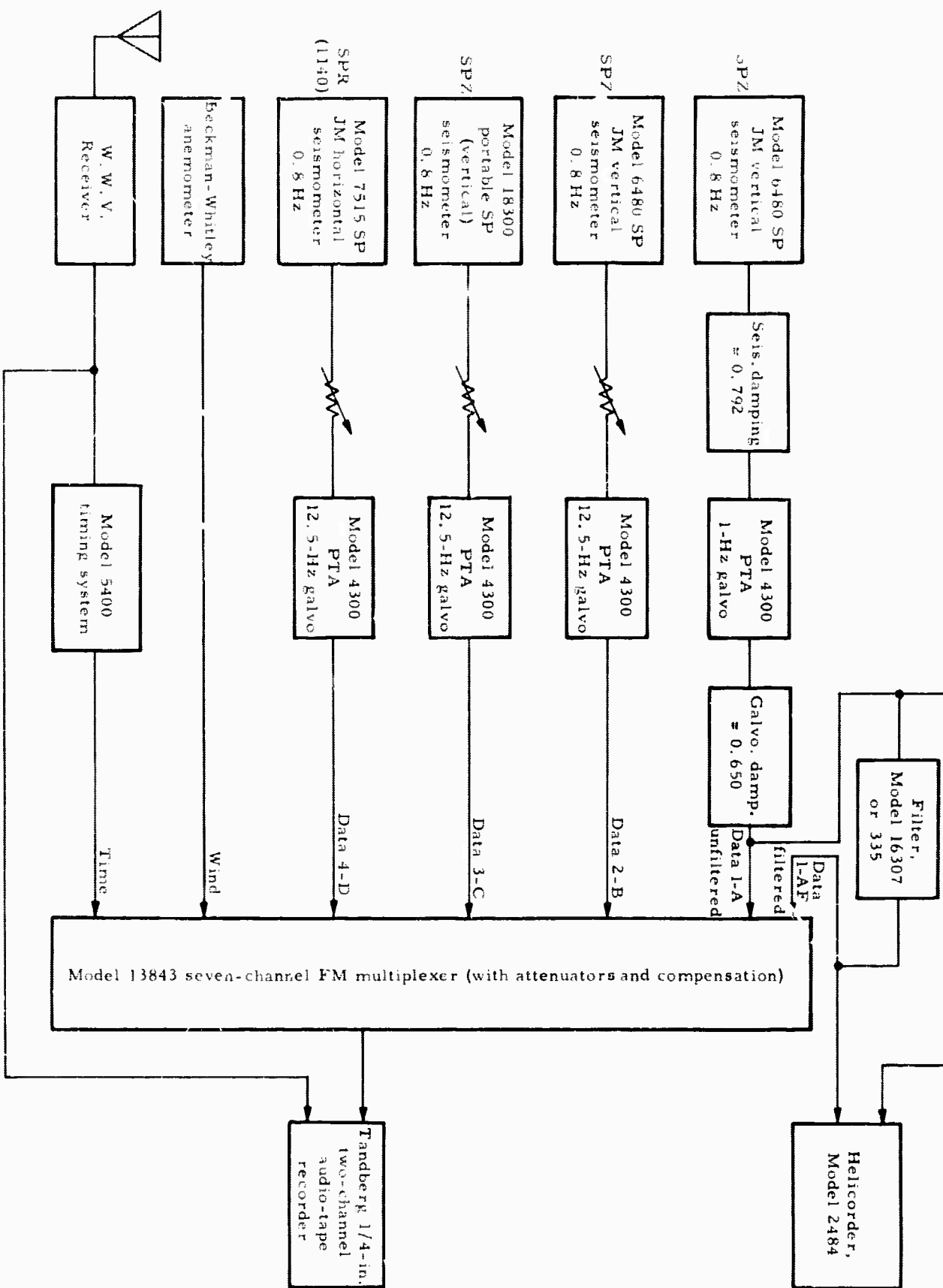


Figure 8. Block diagram of instrumentation used to test and evaluate the narrow-band seismographs at LC-NM

In addition, the instrument trailer was equipped with a WWV receiver and Model 5400 timing system. Data readout for two channels was provided by a Model 2480 Helicorder amplifier. Data were FM multiplexed using a Model 13843 seven-channel multiplexer and recorded on 1/4-in. audio-magnetic tape using a Tandberg tape recorder.

Calibrations were performed using manual and electrical weight lifts; sinusoidal steady-state frequency responses were determined from a pre-recorded calibration tape and a separate Tandberg tape recorder. The frequency response characteristics of the various data channels are shown in figure 9. For reference, the response of the standard LRSM Benioff seismograph is shown. All data are normalized to 1 Hz. The seismometer and galvanometer undamped natural frequencies were determined in the laboratory prior to field installation

On initial installation and at approximately biweekly intervals thereafter, the individual instrument G factors (in newtons/ampere) were determined. Frequency response curves for each instrument were determined initially and at weekly intervals thereafter. The data 2-B, 3-C, and 4-D channels were operated broad-band as "flat velocity fourth order direct-coupled" (Johnson and Matheson, 1962) systems from 0.8 to 12.5 Hz. Datum 1-A was operated narrow-band, 0.8 to 1.0 Hz, with (datum 1-AF) and without (datum 1-A) additional high-pass filtering. Helicorder playout magnifications were determined in the field.

Field tests showed that the Model 16307 variable filter performed better than the Krohn-Hite Filter, Model 335. The Model 335 filter is approximately equivalent to the Model 16307 variable filter and was adjusted to give approximately the same operating characteristics. The advantage of the Model 16307 filter (see figure 10) was the fact that it could be adjusted for critical damping whereas the Model 335 filter could only operate underdamped. The net result was that, while almost as effective in improving the signal-to-noise ratio, the Model 335 filter introduced more signal distortion and was less effective than the Model 16307 variable filter.

Figure 10 shows a teleseism that originated near the New Hebrides Islands ( $\Delta = 95$  deg) as recorded at LC-NM by data 1-A, 1-AF, and 2-B seismographs. This figure shows the sharp beginning of first motion and the distinct P group on the datum 1-AF trace contrasted with the gradual first motion and less distinct P group on data 1-A, 2-B, and 3-C traces. Thus, the good definition of the P phase on the datum 1-AF trace is attributed to the rejection of the 2- to 6-sec microseisms by the Model 16307 filter.

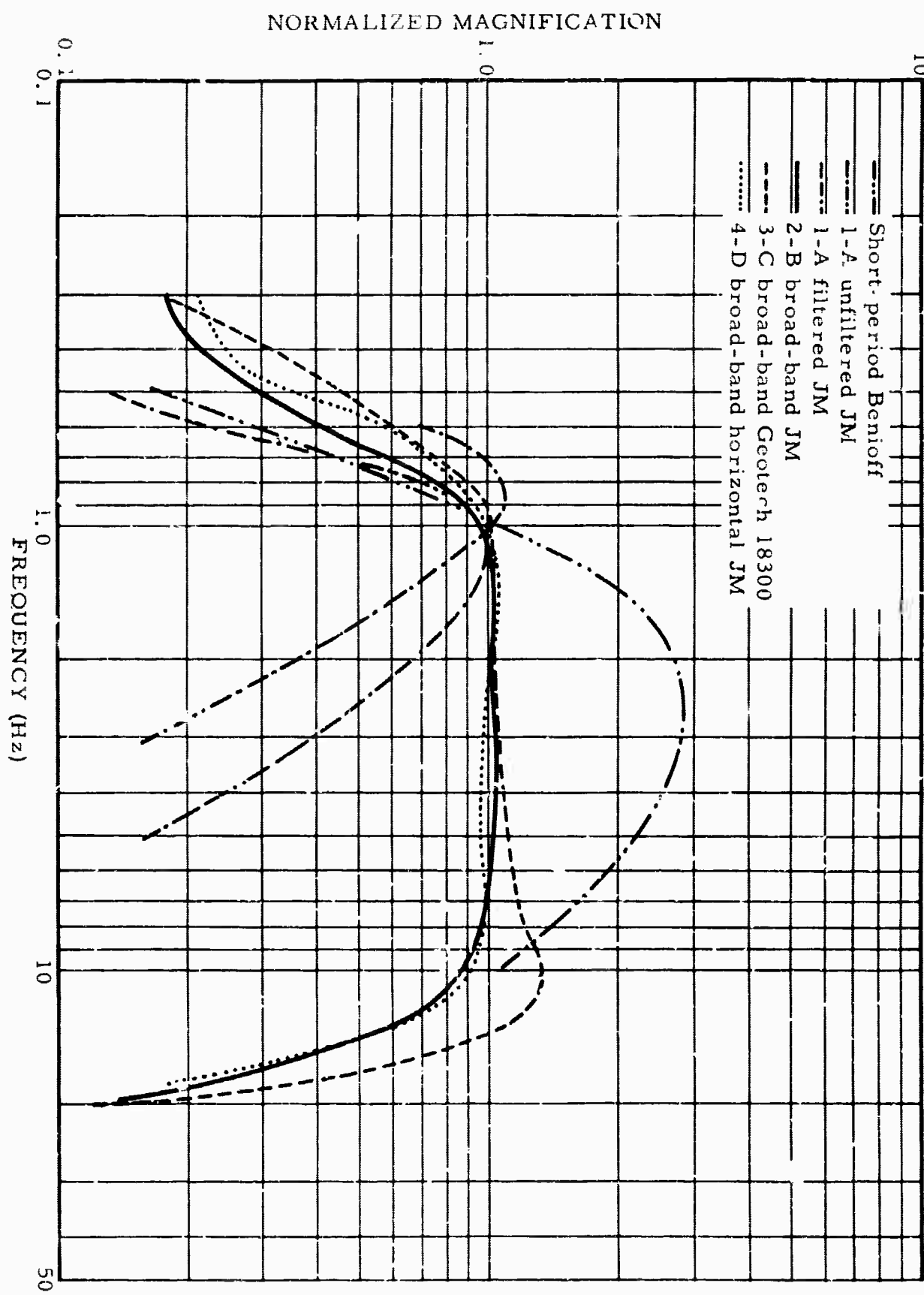


Figure 9. Normalized response characteristics of the seismograph systems used at LC-NM

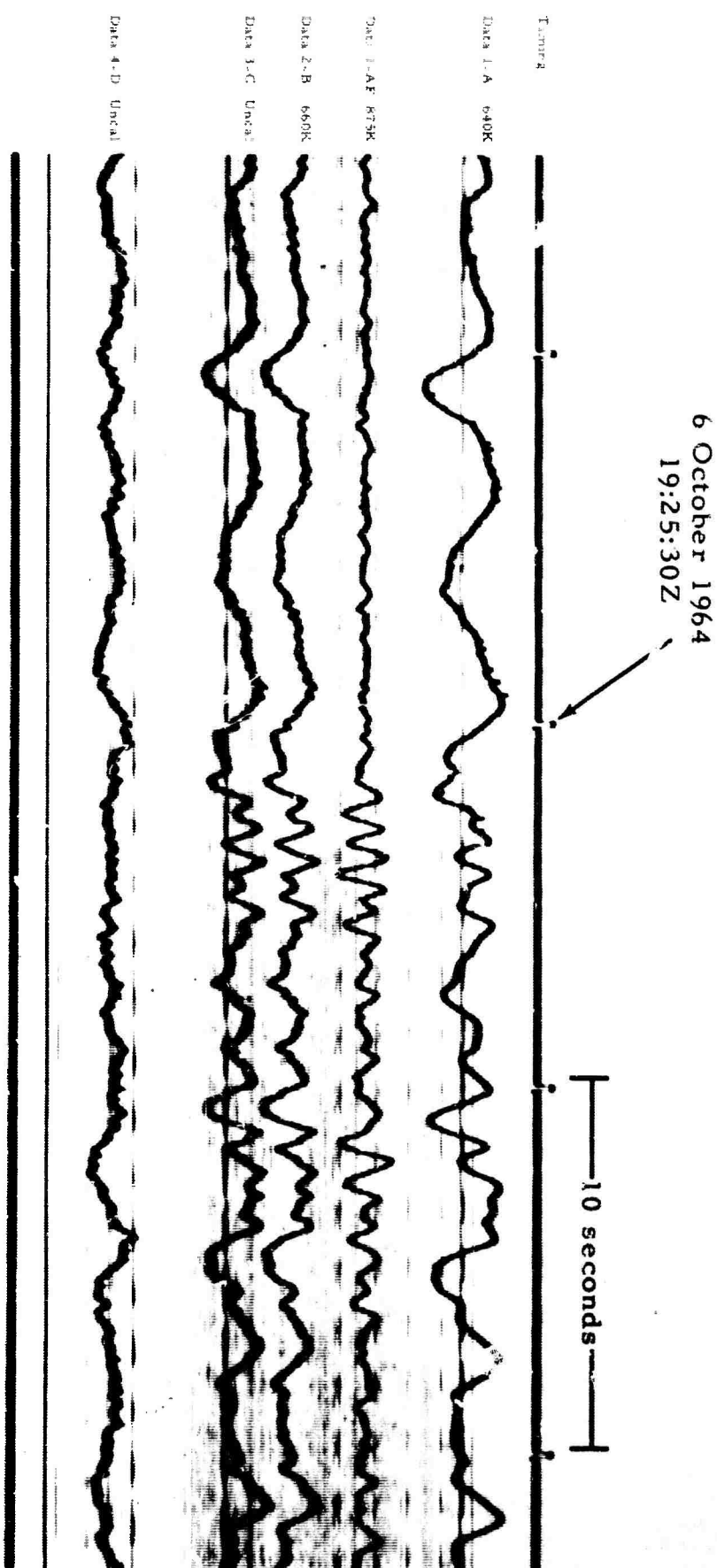


Figure 10. Recording of a P phase from the New Hebrides Islands ( $\Delta = 95$  deg) by data 1-A, 1-AF, 2-B, 3-C, and 4-D seismographs at LC-NM. Magnifications at 1 Hz (X10 enlargement of 16-mm film)

#### 4.4 ANALYSIS OF RECORDED DATA

The signals used in this analysis were obtained from Develocorder recordings of a 1/4-in. magnetic-tape playback. The resulting Develocorder records covered the last 5 days of operation only. Primary arrivals were sampled from the filtered narrow-band seismograph (datum 1-AF), the unfiltered narrow-band seismograph (datum 1-A), and the broad-band seismograph (datum 2-B). Systems were evaluated with regard to primary arrivals only because of the limited number of events. Data recorded on 3-C and 4-D channels were not analyzed. Where data were not available on film, some Helicorder records were used. Data from a short-period Benioff seismometer were also recorded on 35-mm film at Las Cruces, simultaneously but independently of the above systems as part of the LPSC program. Some data from this system were also incorporated in the report.

The actual number of events detected visually on each system by an experienced seismologist was converted to percentages of the total number of events, 30. Percentages are: datum 1-AF, 97 percent; datum 1-A, 80 percent; datum 2-B, 78 percent; and Benioff, 23 percent. The lower percentages of events detected by the Benioff seismograph may be invalid because (a) the Benioff records were analyzed routinely prior to the above analysis, and (b) the output of the Benioff seismometer was not recorded on the Develocorder film used in the above analysis.

As a method of determining the relative visual-detection capabilities of the experimental systems, signal-to-noise ratios were determined with respect to noise in the band of 0.3 to 1.3 sec only. That is, the 2- to 6-sec microseisms were filtered visually by the analyst. The resulting signal-to-noise ratios were plotted against P-wave maximum ground velocity in  $m\mu$  /sec for event, figure 11. This plot shows that events recorded by datum 1-AF have somewhat greater signal-to-noise ratios than data 1-A and 2-B even when the microseisms were visually filtered from the latter two traces. This suggests that the filtering system of datum 1-AF is more effective than the eye in filtering 2- to 6-sec microseisms (see figure 10). Moreover, detection (see percentages above) may be a function of this effective filtering.

#### 4.5 CONCLUSIONS

The following conclusions can be drawn from the small amount of data from LC-NM: (a) the narrow-band seismograph utilizing a Model 16307 filter improves signal-to-noise ratios by minimizing the 2- to 6-sec microseisms, and (b) the filtered narrow-band seismograph appears to improve detection capability.

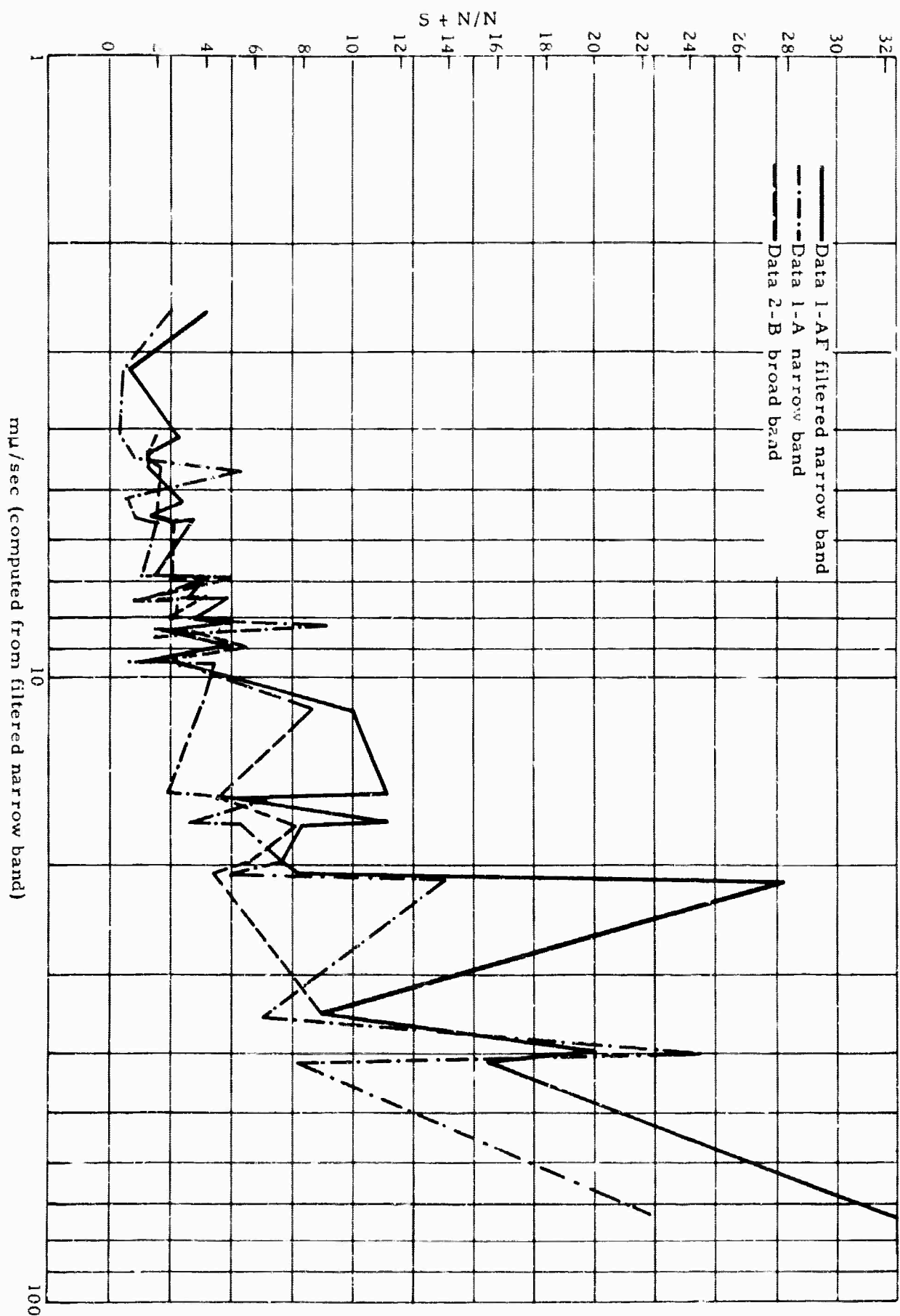


Figure 11. Plot of signal-to-noise ratio versus P-wave maximum ground velocity for 30 events recorded by data 1-AF, 1-A, and 2-B seismographs at LC-NNM.

#### 4.6 RECOMMENDATIONS

A three-component filtered narrow-band seismograph should be operated continuously for a year at LC-NM or at an observatory having similar noise and signal spectra, along with other three-component seismographs that are used in various observatories. The resulting seismic signals and noise should be subjected to detailed visual and spectral analysis.

A possible application for the filtered narrow-band seismograph would be in automated analysis wherein at least one criterion for detection would be that a signal exceed a certain threshold level. Any threshold level set for the broad-band and LRSM seismographs above the long-period noise would miss many of the small signals having amplitudes less than the long-period noise. By using a filtered seismograph, the threshold could be lowered considerably, thereby increasing the number of small signals that could be detected.

#### 4.7 ADMINISTRATION

The personnel listed below developed the filtered narrow-band seismograph, operated the seismograph in the field, analyzed the data, and wrote this section of the report. Dr. Eugene Herrin, associate professor, Southern Methodist University, was consultant for this project.

William Mitcham	Engineer
Kenneth Tiroff	Engineer
David Krug	Research Technician
Richard Kirklin	Seismologist
Herbert Robertson	Geophysicist

#### 4.8 REFERENCES

Johnson, D. P., and Matheson, Harry, 1962, An analysis of inertial seismometer-galvanometer combinations: NBS Report 7454, p. 76.

## 5. HIGHER-MODE RAYLEIGH WAVES

### 5.1 DISCUSSION

Recordings from the deep-hole site at Fort Stockton, Texas, have resulted in seismograms from instruments at depths sufficiently great (up to 5.2 km) that the amplitude-depth relationships of the higher-mode Rayleigh waves can be observed. These Rayleigh waves, as recorded by seismographs of the Benioff type, typically arrive with periods between 2.0 and 4.0 sec. Both the first and second higher modes ( $M_{12}$  and  $M_{21}$ ) have been discussed in the literature (Bath, 1965, and Oliver and Ewing, 1958) for periods greater ( $>5.0$  sec) than the ones at which they are usually recorded by short-period Benioff seismographs.

This study was started with the theory that even higher modes would be present at periods of 2.0 and 3.0 sec. Figure 12 shows a seismogram of a train of 2.0-sec period waves arriving at Fort Stockton with a group velocity of 3.38 km/sec. This group velocity is typical of higher-mode surface waves. The vertical component is very small at 2850 m and 180 deg out-of-phase with the surface at 4572 m.

Figure 13 shows the theoretical amplitude-depth curves of first and second higher-mode Rayleigh waves at this site. The P-wave velocities used in the theoretical model was obtained from a sonic log, and the S velocities and densities were assumed from a knowledge of rocks in the section.

A comparison between figures 12 and 13 points out the difficulties encountered:

a. The experimentally determined nodal point is not in agreement with the theory; the theory indicates that for any higher mode, the wave motion should be out of phase at 2850 m. Both visual examination and spectral analysis indicate that the wave motion is still in phase with the surface at this depth.

b. The experimental amplitudes at 4572 m are not in agreement with the theoretically predicted amplitudes of either mode.

Possible reasons for the disagreement between theory and experiment are being investigated.

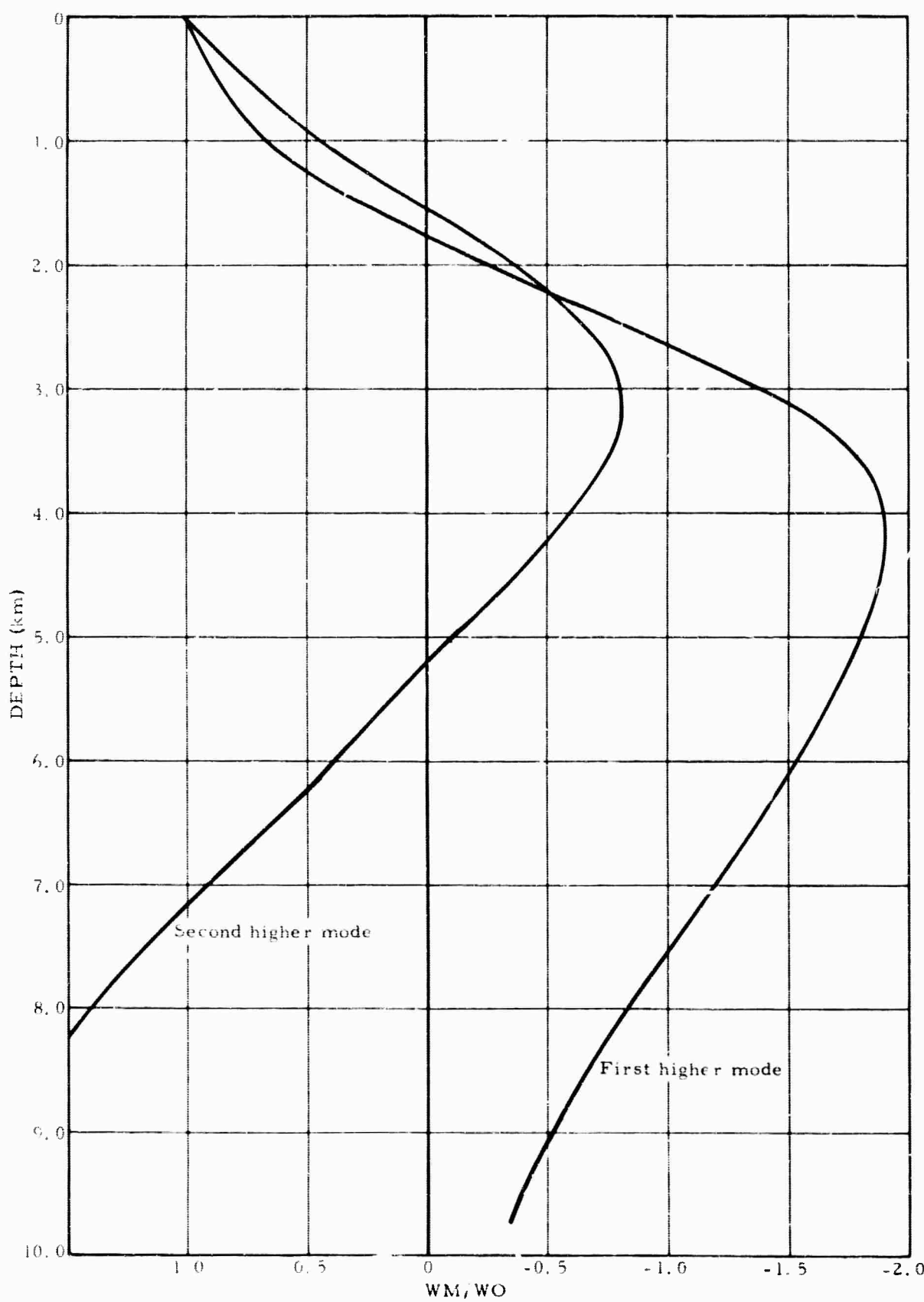


Figure 12. Theoretical amplitude-depth relationships of the first and second higher-mode Rayleigh waves, Fort Stockton, Texas

11 April 1965  
05:06:30Z

10 seconds

WWV

SPZ 358K

DH-3 468K

DH-2 750K

DH-1 896K

SPZ 285K

DH-3 798K

DH-2 1460K

DH-1 1840K

SPR 324K

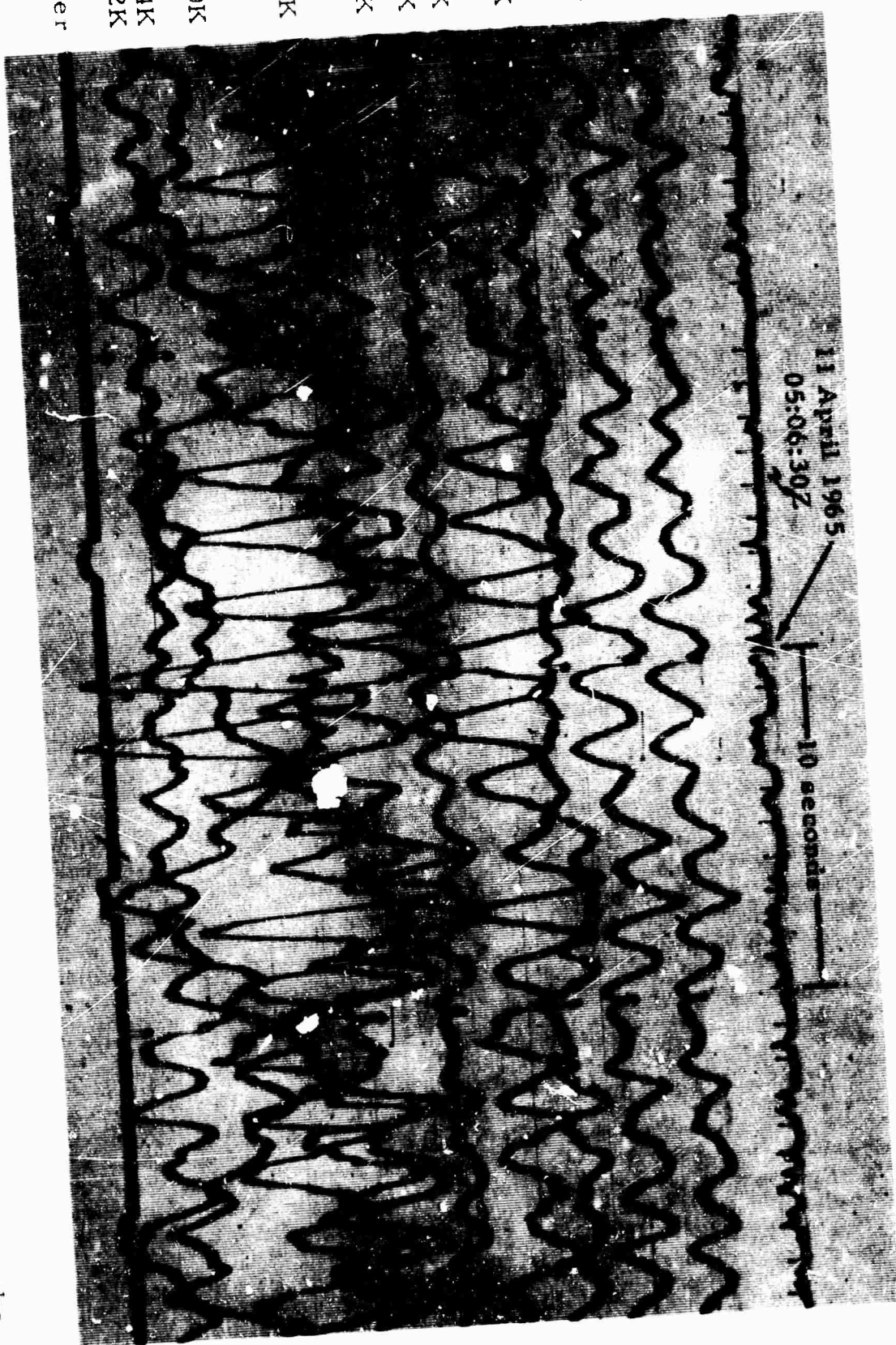
SPT 372K  
Anemometer  
8 km/hr

Figure 13. Recording of an Lg phase from Baja California, by deep-hole and surface seismographs at Fort Stockton, Texas Epicenter 27 N., 115 W. Magnifications at 1 Hz (X10 enlargement of 16-mm film). DH-1 at 4572 m, DH-2 at 2850 m, DH-3 at 60 m

## 5.2 REFERENCES

Bath, M., and Crampin, S., 1965, Higher modes of seismic surface waves: Geophysical Journal, vol. 9, p. 309-321.

Oliver, J., and Ewing, M., 1958, Normal modes of continental surface waves: Bull. Seismol. Soc. Am., vol. 48, p. 33-50.

## 6. SUMMARY

This report describes the work done under Contract AF 49(638)-1150 during the period of 1 January to 30 June 1965.

Of the subjects discussed, the experiment on a filtered narrow-band seismograph was completed. The narrow-band system appears to have a better detection capability than the standard Benioff system at the Las Cruces site.

The study on the statistical properties of the noise will be finished in the near future. Preliminary results show that observed ratios of average peak noise to average noise agree with theoretical ratios derived by Longuet-Higgins for narrow-band ocean waves.

Data analyses of short-period seismic noise is a study that will continue throughout the contract. At present, the major effort is to investigate the presence of body waves in the noise. Body waves have been shown to exist at the Grapevine, Texas, deep-hole site. Available short-period noise data is being investigated to specify the frequencies at which body waves exist.

The study of higher-mode Rayleigh waves from regional earthquakes has only recently been started. Discrepancies between theory and experiment must be resolved before further experimental data will be processed.

APPENDIX to TECHNICAL REPORT NO. 65-77  
PROGRESS REPORT ON SPECIAL ORIENTATION PROGRAM

by

D. C. Rasmussen

## PROGRESS REPORT ON SPECIAL ORIENTATION PROGRAM

### 1. INTRODUCTION

On 1 January 1965, three tasks remained in the Special Orientation Program. These were:

- a. A 2-week phase-in program for the new station operators at the overseas sites;
- b. A 2-week inspection trip of the overseas sites and facilities;
- c. The preparation of an Atlas of Signals from earthquakes recorded at the overseas sites.

### 2. PHASE-IN PROGRAM

During February and March 1965, each of the three overseas sites were visited. In addition to the objectives of providing additional orientation to the new station operators, these trips accomplished the following:

- a. Equipment and vehicle maintenance;
- b. Inventory of tools and equipment;
- c. General site and van clean up;
- d. Coordination of station transfer.

John R. Sherwin, instructor during the orientation program, and supervisor of the overseas teams, conducted this work. Specific details of the work done at each site was documented in trip reports. Transfer of the overseas teams to the Air Force Office of Scientific Research became effective on the following dates:

<u>Site location</u>	<u>Transfer date</u>
La Paz, Bolivia	15 February 1965
Grafenberg, Germany	2 March 1965
Oslo, Norway	1 April 1965

The new station managers indicated their satisfaction with the condition of the equipment prior to the transfer dates. The phase-in task has been completed.

### 3. INSPECTION TRIP

Trips to each site are scheduled for September 1965. The purpose of these trips is to inspect and modify equipment as required and to bring station operators up-to-date on new analysis techniques, station operations, etc.

### 4. ATLAS OF SIGNALS

This task will be 90-percent complete on 1 July 1965. Distribution of the Atlas is scheduled for mid-July. The original schedule called for delivery on 1 June 1965. This delay came about because:

- a. Analysis of a very large volume of seismograms was necessary to find a variety of signals recorded by the European stations;
- b. The time required to secure records from the Seismic Data Laboratory was greater than anticipated.